# Intranuclear Cascade Studies of Low-Energy Pion-Induced Nuclear Reactions: Possible Effects of the Finite Lifetime of the (3,3) Isobar*

G. D. Harp, K. Chen, and G. Friedlander
*Chemistry Department, Brookhaven National Laboratory, Upton, New York 11973*

Z. Fraenkel
*Nuclear Physics Department, Weizmann Institute of Science, Rehovoth, Israel*

J. M. Miller
*Chemistry Department, Columbia University, New York, New York 10027*

(Received 12 February 1973)

Intranuclear cascade studies have been made of low-energy pion-induced nuclear reactions which include the production and subsequent interactions of (3,3) isobars. The results are in fair to excellent agreement with the sparse amount of experimental information now available. Several experiments are outlined which could test the validity of some of the assumptions which were made in these calculations.

## I. INTRODUCTION

A number of intranuclear cascade studies of high-energy reactions have been made which utilize the Sternheimer-Lindenbaum isobar model[1] for pion production in inelastic pion-nucleon and nucleon-nucleon collisions within the nucleus.[2,3] This model assumes that one or more (3, 3) isobars are produced in such collisions. In the above cascade studies it is assumed that these isobars decay immediately after their formation. That is, the possibility of their interaction with other nucleons in the target is assumed to be negligible. Moreover, both in the above studies and in other cascade studies involving low-energy pions[2,4-6] it is assumed that (3, 3) isobars formed in elastic pion-nucleon collisions within the nucleus also decay immediately after formation.

However, if this isobar was produced within a nucleus in an intranuclear cascade then there is the distinct possibility that it could interact with another nucleon or a cluster of nucleons before decaying. This is due to the fact that the time between two successive collisions of a cascade particle is the same order of magnitude as this isobar's mean lifetime ($\sim 0.73\times10^{-23}$ s in its own c.m. system).[7] Further, since one of the decay products of a (3, 3) isobar is a nucleon, the isobar lifetime in a nucleus is increased by the Pauli principle. Finally, if the isobar has high kinetic energy then its lifetime is further increased by relativistic time dilation.

Fraenkel proposed two possible isobar-nucleon interactions[7,8]:

*1. Isobar capture.* Schematically this process may be written as

$$\Delta + N_1 \rightarrow N_2 + N_3 , \tag{1}$$

where $\Delta$ is an isobar and $N$ is a nucleon. The characteristics of this process have been calculated from its inverse: isobar production in inelastic nucleon-nucleon collisions.[7] Notice that if an isobar is formed in an elastic pion-nucleon interaction and then interacts with another nucleon by the above process, the net result is the capture of the initial pion by a pair of nucleons. This two-step process for pion absorption in complex nuclei differs from that previously employed in intranuclear cascade calculations in a number of respects. Perhaps the most important difference is that this two-step process provides a mechanism for the absorption of high-energy pions. However, neither this mechanism for pion absorption nor that previously used considers more than two nucleons as being important in the absorption process.

*2. Isobar-nucleon "exchange" scattering.* Schematically this process may be written as

$$\Delta_1 + N_1 \rightarrow \Delta_2 + N_2 . \tag{2}$$

In this type of interaction both the charge and mass of the isobar may change.

In the light of the above, it is of interest to perform intranuclear cascade studies in which (3, 3) isobars are produced and are not only allowed to decay but are also allowed to interact with other nucleons in the nucleus. Good agreement between the results of such calculations and experiment could then be used to support the view that isobars exist for a finite period of time in complex nuclei during high-energy reactions. In addition, such calculations could test the validity of the tacit assumption made in previous intranuclear cascade studies that isobar-nucleon interactions are relatively unimportant.

## II. DETAILS OF MODEL

The model that was used is an extensively modified version of an intranuclear cascade calculation for medium-energy, nucleon-induced nuclear reactions. Since this calculation is described in great detail elsewhere,[9] only a brief description of it, as well as those changes that were made to handle the present problem, will be given here.

The nuclear radial density distribution is represented by a series of steps. This step density distribution is equivalent to a series of concentric regions each having a constant but different density. The potential which acts on the cascade neutrons (protons) in a particular region is the sum of the neutron (proton) Fermi energy in that region and the average binding energy of the last few nucleons in the nucleus. The refraction or reflection of cascade particles at potential boundaries is neglected.

Another more physically realistic model has been developed which uses a velocity-dependent potential, refracts or reflects nucleons at potential boundaries, and attempts to approximate the effects of nucleon pair correlations in the target nucleus on cascade nucleons.[10] However, the results obtained from these two models are in excellent agreement with one another. Therefore, the logically simpler model was used here.

The pion-nucleus potential was assumed to be constant and attractive. No attempt was made to use a more complex interaction potential such as the velocity- and density-dependent Kisslinger potential.[11]

The isobar-nucleus interaction potentials were arbitrarily assigned as follows: a positively charged isobar was assigned a potential equal to the sum of proton and pion potentials while the potential assigned to a negatively charged or neutral isobar was the sum of neutron plus pion potentials.

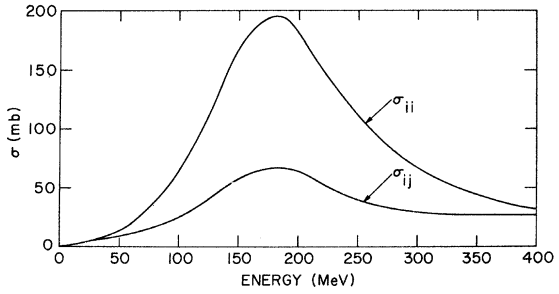


FIG. 1. Pion-nucleon total cross sections. $\sigma_{ii}$ is the cross section for either $\pi^+$-$p$ or $\pi^-$-$n$ interactions and $\sigma_{ij}$ is the cross section for either $\pi^+$-$n$ or $\pi^-$-$p$ interactions. The curves are based on the experimental cross sections compiled in Ref. 12.

In the present model pion-nucleon interactions can only produce $T=\frac{3}{2}$ isobars. The cross sections that were used for this process are the experimental, elementary pion-nucleon total (elastic plus charge exchange) cross sections[12] presented in Fig. 1. In this figure $\sigma_{ii}$ is the cross section for either $\pi^+$-$p$ or $\pi^-$-$n$ interactions and $\sigma_{ij}$ is the cross section for either $\pi^+$-$n$ or $\pi^-$-$p$ interactions. From isotopic spin considerations the cross section for $\pi^0$-$n$ or $\pi^0$-$p$ interactions is taken to be the arithmetic mean of $\sigma_{ii}$ and $\sigma_{ij}$. Although the model assumed only the formation of $T=\frac{3}{2}$ isobars, the energy region considered actually brought in a contribution from the $T=\frac{1}{2}$ state. Thus, particularly at the high energies, $\sigma_{ij}$ was taken from experimental values rather than from isotopic spin considerations.

The physical properties of an isobar produced in a pion-nucleon interaction were determined from the appropriate characteristics of the pion-nucleon system from which it was formed. These properties include the $T_Z$ component of the isotopic spin as well as the mass, energy, and momentum of the isobar.

The mean free path for isobar decay, $\lambda_D$, is given by

$$\lambda_D=\frac{\beta_\Delta c\tau}{(1-\beta_\Delta^2)^{1/2}}, \tag{3}$$

where $c$ is the velocity of light, $\beta_\Delta$ is the velocity of the isobar in units of $c$, and $\tau$ is the mean lifetime of the (3, 3) isobar in its c.m. system. $\tau$ was assumed to be $0.73\times10^{-23}$ sec.[7]

The branching ratios that were used for isobar decay were those dictated by isotopic spin considerations. For example, the probability that a charged pion and a nucleon are produced in the decay of either a $T_Z=\frac{1}{2}$ or a $T_Z=-\frac{1}{2}$ isobar is $\frac{1}{3}$.

In the present model the formation of an isobar followed by its decay is equivalent to an elastic or charge exchange scattering of the pion and nucleon which originally formed the isobar. This two-step mechanism for pion-nucleon scattering must be entirely equivalent to pion-nucleon scattering in free space. In order to satisfy this constraint the angular distributions used in isobar decay were either the c.m. elastic or the c.m. charge-exchange scattering distributions for the pion and nucleon originally forming the isobar. These latter distributions were obtained from the experimental c.m. elastic $\pi^+$-$p$, and c.m. elastic and charge exchange $\pi^-$-$p$ differential scattering cross sections[12] by first fitting these cross sections at several energies to functions of the form $A\cos^2\theta_{\text{c.m.}}+B\cos\theta_{\text{c.m.}}+C$ where $\theta_{\text{c.m.}}$ is the c.m. scattering angle of the pion. The resulting plots of $A$, $B$, and $C$ versus $T_u$, the pion-nucleon c.m.

kinetic energy, were then smoothed by hand such that the final coefficients were continuous functions of $T_u$. The $\pi^0$-$p$ or $\pi^0$-$n$ elastic differential cross section was calculated from the previous cross sections by the following expression which is derived from isotopic spin considerations:

$$\frac{d\sigma^{el}}{d\Omega}(\pi^0\text{-}n) = \frac{d\sigma^{el}}{d\Omega}(\pi^0\text{-}p) = \frac{1}{2}\left[\frac{d\sigma^{el}}{d\Omega}(\pi^-\text{-}p) + \frac{d\sigma^{el}}{d\Omega}(\pi^+\text{-}p) - \frac{d\sigma^{ex}}{d\Omega}(\pi^-\text{-}p)\right], \quad (4)$$

where $(d\sigma^{el}/d\Omega)(\pi\text{-}N)$ and $(d\sigma^{ex}/d\Omega)(\pi\text{-}N)$ are the $\pi$-$N$ elastic and charge exchange differential scattering cross sections, respectively. If an isobar interacted with a nucleon before decaying then it was forced to decay isotropically in its own c.m. system.

Only two types of isobar-nucleon interactions were considered: isobar capture and isobar-nucleon "exchange" scattering. The total and differential cross sections used for the first process are discussed in great detail elsewhere.[7]

The general theory pertaining to the calculation of the total and differential cross sections used for the second process is given in Ref. 8. Naively, one can view isobar-nucleon "exchange" scattering as a two-step process: the decay of the initial isobar followed by the interaction of the decay pion with the initial nucleon to form the final isobar. Therefore, both the mass and charge of the initial and final isobars may be different. However, in order to simplify matters somewhat, it was assumed that only the charge may change. The cross sections for the "exchange" scattering of a $T_Z = \frac{3}{2}$ isobar of mass 1.238 GeV from a stationary proton are given in Table I. "Exchange" scattering cross sections depend somewhat on the mass of the initial isobar. However, this dependence was neglected. That is, the cross sections in Table I were used for all initial isobar masses. These cross sections are actually the total cross sections for the above reaction in the sense that they include the production of all kinematically allowed, final isobar masses. However, they were used in the present model for "exchange" scattering in which the mass of the isobar was the same before and after collision. The cross sections for the other possible isobar-nucleon "exchange" reactions are proportional to the cross section for the preceding reaction. The appropriate proportionality constants are given in Table II.

The c.m. differential cross section for isobar-nucleon "exchange" scattering is proportional to $[(A\cos\theta + B + 0.196)^2 + 10^{-2}C]^{-1}$, where $\theta$ is the angle between the initial and final isobars in the c.m. The coefficients $A$, $B$, and $C$ are functions of the total c.m. energy and the masses of the nucleons and isobars involved in the scattering. These coefficients are given in Table III for the scattering of an isobar from a nucleon in which the initial and final isobar masses are both 1.238 GeV. Notice that these cross sections have a maximum for $\cos\theta = -(B + 0.196)/A$.

It was assumed that both the total and differential cross sections for isobar-nucleon "exchange" scattering were independent of the initial isobar mass. Therefore, the data in Table I (multiplied

TABLE I. Isobar-nucleon "exchange" cross sections for the reaction: $\Delta(T_Z = \frac{3}{2}) + p \rightarrow \Delta(T_Z = \frac{3}{2}) + p$. The initial isobar mass is 1.238 GeV, i.e., the most probable isobar mass.

| $E_{lab}$ [a] (MeV) | $\sigma$ (mb) | $E_{lab}$ [a] (MeV) | $\sigma$ (mb) |
|---|---|---|---|
| 50 | 216.1 | 550 | 84.9 |
| 100 | 192.6 | 600 | 79.7 |
| 150 | 172.4 | 650 | 74.9 |
| 200 | 153.5 | 700 | 70.7 |
| 250 | 137.8 | 750 | 67.1 |
| 300 | 124.8 | 800 | 63.7 |
| 350 | 114.3 | 850 | 60.7 |
| 400 | 105.4 | 900 | 57.9 |
| 450 | 97.7 | 950 | 55.3 |
| 500 | 90.9 | 1000 | 53.1 |

[a] $E_{lab}$ is the laboratory kinetic energy of the initial isobar striking a stationary proton.

TABLE II. The squares of the relative amplitudes for all isobar-nucleon "exchange" reactions.

| Reaction | Square of relative amplitude |
|---|---|
| $\Delta(T_Z = \frac{3}{2}) + p \rightarrow \Delta(T_Z = \frac{3}{2}) + p$ | 1 |
| $\Delta(T_Z = \frac{3}{2}) + n \rightarrow \Delta(T_Z = \frac{1}{2}) + p$ | $\frac{1}{3}$ |
| $\Delta(T_Z = \frac{1}{2}) + p \rightarrow \Delta(T_Z = \frac{1}{2}) + p$ | $\frac{4}{9}$ |
| $\Delta(T_Z = \frac{1}{2}) + p \rightarrow \Delta(T_Z = \frac{3}{2}) + n$ | $\frac{1}{3}$ |
| $\Delta(T_Z = \frac{1}{2}) + n \rightarrow \Delta(T_Z = -\frac{1}{2}) + p$ | $\frac{4}{9}$ |
| $\Delta(T_Z = \frac{1}{2}) + n \rightarrow \Delta(T_Z = \frac{1}{2}) + n$ | $\frac{1}{9}$ |
| $\Delta(T_Z = -\frac{1}{2}) + n \rightarrow \Delta(T_Z = -\frac{1}{2}) + n$ | $\frac{4}{9}$ |
| $\Delta(T_Z = -\frac{1}{2}) + n \rightarrow \Delta(T_Z = -\frac{3}{2}) + p$ | $\frac{1}{3}$ |
| $\Delta(T_Z = -\frac{1}{2}) + p \rightarrow \Delta(T_Z = \frac{1}{2}) + n$ | $\frac{4}{9}$ |
| $\Delta(T_Z = -\frac{1}{2}) + p \rightarrow \Delta(T_Z = -\frac{1}{2}) + p$ | $\frac{1}{9}$ |
| $\Delta(T_Z = -\frac{3}{2}) + p \rightarrow \Delta(T_Z = -\frac{1}{2}) + n$ | $\frac{1}{3}$ |
| $\Delta(T_Z = -\frac{3}{2}) + n \rightarrow \Delta(T_Z = -\frac{3}{2}) + n$ | 1 |

TABLE III. The coefficients in the c.m. differential cross section for isobar-nucleon "exchange" scattering in which the initial and final isobar masses are 1.238 GeV. The coefficients are in arbitrary units and $U$ is the total c.m. energy.

| $U$ (GeV) | $A$ | $B$ | $C$ | $U$ (GeV) | $A$ | $B$ | $C$ |
|---|---|---|---|---|---|---|---|
| 2.297 | 2.660 | 1.852 | 6.020 | 2.492 | 7.269 | 6.582 | 4.493 |
| 2.317 | 3.114 | 2.321 | 5.837 | 2.511 | 7.739 | 7.063 | 4.371 |
| 2.337 | 3.573 | 2.793 | 5.660 | 2.530 | 8.213 | 7.547 | 4.253 |
| 2.357 | 4.036 | 3.269 | 5.490 | 2.549 | 8.690 | 8.034 | 4.139 |
| 2.377 | 4.503 | 3.749 | 5.327 | 2.567 | 9.146 | 8.499 | 4.035 |
| 2.397 | 4.974 | 4.232 | 5.169 | 2.585 | 9.605 | 8.967 | 3.933 |
| 2.416 | 5.425 | 4.695 | 5.024 | 2.603 | 10.07 | 9.439 | 3.835 |
| 2.435 | 5.881 | 5.162 | 4.885 | 2.621 | 10.53 | 9.913 | 3.740 |
| 2.454 | 6.340 | 5.632 | 4.750 | 2.639 | 11.00 | 10.39 | 3.647 |
| 2.473 | 6.802 | 6.105 | 4.619 | 2.656 | 11.45 | 10.84 | 3.563 |

by the appropriate constants in Table II) were used for the total cross sections, and the data in Table III were used for the angular distributions. Parabolic interpolation was used for points not in these tables.

The potential energy may change in isobar formation or in isobar scattering. The total energy is conserved in all such interactions by appropriately changing the relative kinetic energy in the c.m. of the colliding particles.

## III. COMPARISON AMONG MODELS AND WITH EXPERIMENTAL DATA

At the present time there are insufficient experimental data available to adequately test the various assumptions in the present model. Hence, one of the objectives of this section is to pinpoint those areas which are sensitive to these assumptions and which may be examined experimentally in the near future. Of particular interest in this respect is the effect of isobar-nucleon "exchange" scattering, since this interaction has no counterpart in previous intranuclear cascade calculations. Therefore, in the following, results will be presented from calculations in which isobar-nucleon "exchange" scattering is included and neglected. For the sake of brevity, ISONEX shall refer to the model in which "exchange" scattering is included and ISONEX-NO shall refer to the model in which this interaction is neglected.

### A. Determination of the Pion-Nucleus Potential

The pion-nucleus potential was determined empirically by varying the magnitude of this potential and comparing the calculated results to two experimental quantities: the reaction cross section for the interaction of negative pions with $^{12}C$ and the energy spectrum of negative pions which have been inelastically scattered in the backward hemisphere by heavy emulsion nuclei.

The negative pion-$^{12}C$ reaction cross section is particularly suited for this purpose since the calculated cross section is not sensitive to the details of the cascade process but is very sensitive to the magnitude of the pion-nucleus potential used. In Fig. 2 the recent experimental data of Binon *et al.*[13] for negative pion-$^{12}C$ reaction cross sections are compared with two sets of calculated

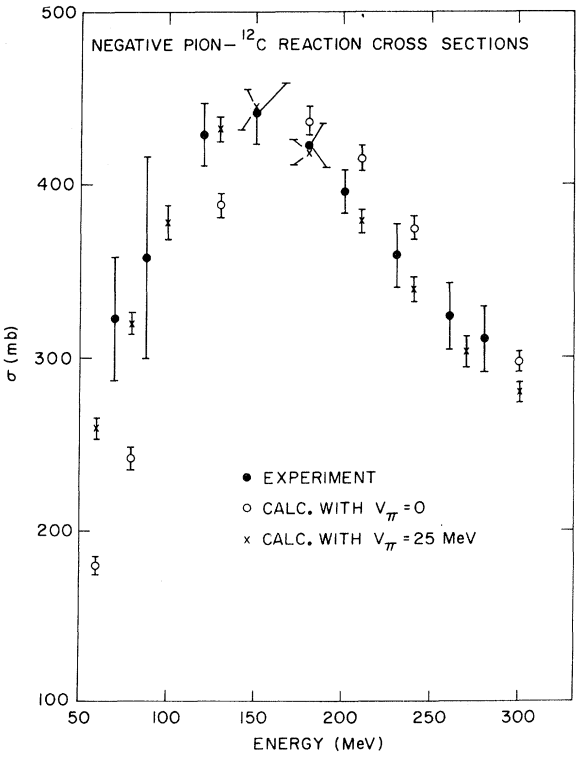


FIG. 2. Calculated and experimental reaction cross sections for the interaction of negative pions with $^{12}C$. The experimental data are taken from Ref. 13.

results: one in which no pion-nucleus potential was used ($V_\pi = 0$) and the other in which an attractive potential of 25 MeV was used ($V_\pi = 25$ MeV). The calculated cross sections for $V_\pi = 25$ MeV are in excellent agreement with experiment over the entire energy range considered. The other set of calculated cross sections differ from the experimental results, especially for incident pion energies less than 180 MeV.

It is unfortunate that precise data on pion-nucleus reaction cross sections are not yet available for nuclei heavier than $^{12}C$. If they were, then one might have greater confidence in the form and magnitude of the pion-nucleus potential used in the present calculation.

Bertini[2,4] has reported a few low-energy pion-nucleus reaction cross sections which were calculated using a different form of the pion-nucleus interaction potential. In general, his results are somewhat larger than those obtained from the present calculation with $V_\pi = 25$ MeV, except for the interaction of negative pions with Pb. In this latter case, the results obtained from the two calculations are essentially identical.

Another piece of experimental information which is available and which is sensitive to the pion-nucleus potential is the energy spectrum of negative pions which have been emitted in the backward direction in the interaction of 162-MeV negative pions with heavy emulsion nuclei.[14] In Fig. 3 the observed energy spectrum is compared with two calculated spectra. Both of these latter spectra were calculated with the ISONEX model, with $V_\pi = 0$ in one calculation and $V_\pi = 25$ MeV in the other. The calculated spectrum for $V_\pi = 25$ MeV is in satisfactory agreement with experiment. The calculated spectrum with no pion-nucleus potential clearly yields too many high-energy pions. In view of the rather poor statistics for the experimental spectrum, perhaps the average kinetic energy of the negative pions which were emitted in the backward direction is a more meaningful measure of the agreement between calculation and experiment. The experimental value of this quantity is $64 \pm 3$ MeV while[14] the calculated values for $V_\pi = 25$ MeV and $V_\pi = 0$ are 62 and 83 MeV, respectively. Clearly, a constant attractive pion-nucleus potential of 25 MeV is needed to reproduce this experimental spectrum. Nikol'skii *et al.*,[14] Metropolis *et al.*,[5] and Barashenkov *et al.*[6] arrived at essentially this same conclusion using intranuclear cascade models which were different from the present one.

One might have assumed that the calculated spectra were sensitive not only to the pion-nucleus potential but also to other details of the particular model used. However, the spectra obtained from the present model are unaffected by isobar-nucleon "exchange" scattering and Barashenkov *et al.*[6] found that their spectra are rather insensitive to the presence or absence of a mechanism for pion absorption. On the other hand, Bertini[4] found that his spectra are sensitive to the nucleon density distributions used in his calculations. In view of the preceding remarks, more precise experimental data on the energy spectra of pions

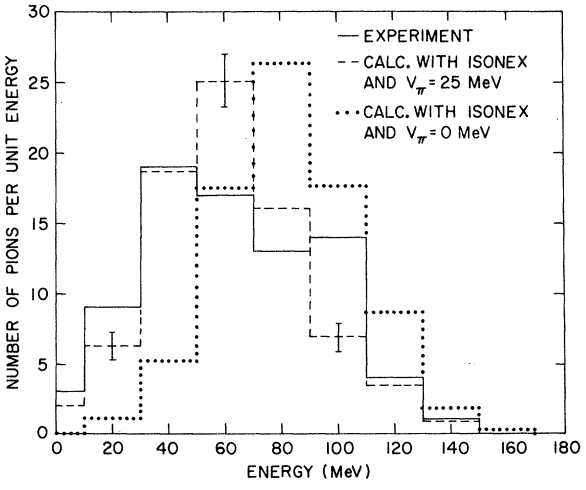


FIG. 3. Energy spectra of negative pions emitted in the backward hemisphere in the interaction of 162-MeV negative pions with heavy emulsion nuclei. The experimental data of Ref. 14 are compared with the calculated results for $^{100}Ru$.

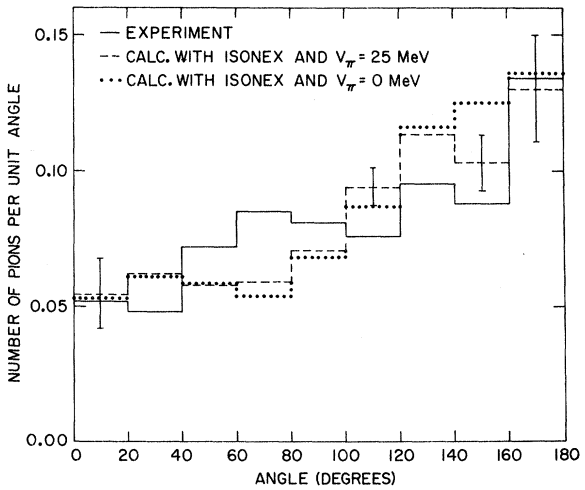


FIG. 4. Angular distributions of negative pions emitted in the interaction of 162-MeV negative pions with heavy emulsion nuclei. The experimental data of Ref. 14 are compared with the calculated results for $^{100}Ru$.

emitted in inelastic interactions of incident pions with heavy nuclei would also be valuable for assigning the pion-nucleus potential in this calculations.

Before proceeding further, the angular distribution of inelastically scattered negative pions, which was measured in the experiment described above, will now be discussed. In Fig. 4, the experimental distribution[14] is again compared with two calculated distributions. Again, both of these latter distributions were calculated with the ISONEX model with $V_\pi = 0$ in one calculation and $V_\pi = 25$ MeV in the other. The calculated distributions are insensitive to the magnitude of the pion-nucleus potential and are in agreement with experiment. However, Barashenkov *et al.*[6] found that their calculated distributions were weakly sensitive to this potential while Metropolis *et al.*[5] found a strong dependence. In fact, these latter authors were unable to fit simultaneously the experimental energy spectrum mentioned above and this angular distribution with any value of the pion-nucleus potential. Metropolis *et al.*[5] suggested that the source of their difficulty was the nucleon density distribution used in their calculations (i.e., a uniform distribution). In particular, they suggested that if they had used a density distribution with a diffuse edge then they would have obtained better agreement with experiment.

TABLE IV. Average excitation energies of residual nuclei produced in the interaction of pions with $^{209}$Bi. $T_\pi$ is the kinetic energy of the incident pion. $\bar{E}^*$ is the average excitation energy of all residual nuclei, while $\bar{E}^*_C$ and $\bar{E}^*_{N.C.}$ are the average excitation energies of nuclei produced in pion capture and noncapture events, respectively. $\bar{n}_{ex}$ is the average number of isobar-nucleon "exchange" scatterings per inelastic cascade. All energies are in MeV.

| | | | $\pi^-$ | | | | |
|---|---|---|---|---|---|---|---|
| | ISONEX | | | | ISONEX-NO | | |
| $T_\pi$ | $\bar{E}^*$ | $\bar{E}^*_{N.C.}$ | $\bar{E}^*_C$ | $\bar{n}_{ex}$ | $\bar{E}^*$ | $\bar{E}^*_{N.C.}$ | $\bar{E}^*_C$ |
| 100 | 62.6 | 26.9 | 94.5 | 0.26 | 59.1 | 27.3 | 91.2 |
| 150 | 74.9 | 35.7 | 107.6 | 0.38 | 71.9 | 35.2 | 104.5 |
| 200 | 98.3 | 44.4 | 129.5 | 0.53 | 90.6 | 39.2 | 120.4 |
| 250 | 117.7 | 51.7 | 149.6 | 0.70 | 107.8 | 44.2 | 138.0 |
| 300 | 137.1 | 59.1 | 170.5 | 0.89 | 122.4 | 42.5 | 156.1 |
| | | | $\pi^+$ | | | | |
| | ISONEX | | | | ISONEX-NO | | |
| $T_\pi$ | $\bar{E}^*$ | $\bar{E}^*_{N.C.}$ | $\bar{E}^*_C$ | $\bar{n}_{ex}$ | $\bar{E}^*$ | $\bar{E}^*_{N.C.}$ | $\bar{E}^*_C$ |
| 100 | 71.4 | 29.7 | 97.4 | 0.21 | 68.7 | 28.8 | 96.7 |
| 150 | 78.2 | 36.2 | 110.3 | 0.31 | 78.7 | 37.9 | 108.1 |
| 200 | 98.4 | 47.7 | 129.5 | 0.46 | 96.0 | 46.0 | 123.7 |
| 250 | 120.1 | 52.6 | 149.1 | 0.55 | 110.6 | 43.0 | 138.1 |
| 300 | 136.7 | 55.5 | 169.4 | 0.65 | 125.1 | 44.3 | 155.4 |

It appears that they were correct in their reasoning since, in the present calculations and in those of Barashenkov *et al.*,[6] diffuse-edge nucleon density distributions are used and neither of these calculations has any difficulty in simultaneously fitting energy and angular distributions.

The present calculation shows that the calculated angular distributions are insensitive to the presence or absence of isobar-nucleon "exchange" scattering. In addition, Barashenkov *et al.*[6] found that their calculated distributions are only weakly sensitive to the presence or absence of a mechanism for pion absorption. On the other hand, Bertini[4] found that his calculated distributions are sensitive to the nucleon density distributions used in his calculations which is in agreement with the preceding discussion of the results of Metropolis *et al.*[5]

The results obtained with the present model using a constant attractive pion-nucleus potential of 25 MeV are in good agreement with the experimental data to which they were compared. Therefore, in the following, only calculated results in which this pion-nucleus potential was used will be reported.

### B. Average Excitation Energies

In this section the average excitation energies of residual nuclei produced in pion-nucleus interactions will be discussed. Pions may transfer their energy to nuclei via inelastic scattering and/or absorption. Hence, it is of interest to examine the average excitation energy of: (a) all residual nuclei produced in pion-nucleus interactions; (b) those nuclei produced in absorption or capture events (i.e., events in which no pions are emitted); and (c) those nuclei produced in noncapture events. These three excitation energies will be denoted by $\bar{E}^*$, $\bar{E}^*_C$, and $\bar{E}^*_{N.C.}$, respectively.

The average excitation energies of residual nuclei produced in the interactions of pions with $^{209}$Bi are presented in Table IV. In addition, this table contains the average number of isobar-nucleon "exchange" scattering per inelastic cascade, $\bar{n}_{ex}$, which will prove useful in the following discussion.

It is informative to first compare the $\bar{E}^*$ values for incident pions with those calculated for incident nucleons. One might have assumed that the $\bar{E}^*$ values for the two types of particle would be comparable provided the kinetic energy of the incident nucleon was equal to the total energy of the incident pion. However, this assumption does not seem to be universally valid. For example, the calculated $\bar{E}^*$ values for residual nuclei produced in the interactions of 240- and 375-MeV pro-

tons with $^{209}$Bi are 96 and 117 MeV, respectively. Although the latter value agrees fairly well with the 250-MeV $\pi^+$ results, the former value is ~26 MeV higher than the 100-MeV $\pi^+$ results and ~35 MeV higher than the 100-MeV $\pi^-$ results.

Note that the $\bar{E}^*$ values for low-energy, incident $\pi^+$'s are slightly larger than the corresponding values for $\pi^-$'s. However, as the bombarding energy increases the differences between these excitation energies vanish. This behavior is partially due to the absorption mechanism employed in the present model. That is, in nuclei for which $A>2Z$ the initial isobars formed in $\pi^+$-nucleon interactions have a greater probability for absorption than those formed in $\pi^-$-nucleon interactions. Hence, for such nuclei one would expect more absorption and, consequently, larger $\bar{E}^*$ values for incident $\pi^+$'s than for incident $\pi^-$'s. This is true provided only one isobar is formed, on the average, in an inelastic cascade as is the case for low-energy but not for high-energy incident pions. In the latter case multiple pion-nucleon scattering becomes important and one would not expect to see much difference between the $\pi^+$ and $\pi^-$ absorption probabilities. An obvious corollary to the above is that there should be very little difference between the $\bar{E}^*$ values for $\pi^+$'s and $\pi^-$'s on light and medium nuclei, irrespective of the incident pion energy. This is indeed what is found.

Note that the $\bar{n}_{ex}$ values increase with bombarding energy and are larger for $\pi^-$'s than for $\pi^+$'s at the same incident energy. The first effect is simply a consequence of an increase in the average number of pion-nucleon collisions with increasing pion energy and thus an increase in the number of isobars involved in an inelastic cascade. For the same reason, one would expect the frequency of "exchange" scattering to increase with the mass of the target. This is indeed what is found. The second effect follows from a rather simple analysis based on the data in Table II and the isobar formation probabilities for incident $\pi^+$'s and $\pi^-$'s. That is, in nuclei for which $A>2Z$ this analysis shows that "exchange" scattering should occur more frequently for incident $\pi^-$'s than for $\pi^+$'s. However, in nuclei for which $A=2Z$ the frequency of "exchange" scattering should be independent of the charge of the incident pion, which is indeed the case.

The average excitation energies obtained from the ISONEX model are, in general, greater than the corresponding energies obtained from the ISONEX-NO model. This effect is particularly noticeable for high incident energies and has a rather simple explanation. When "exchange" scattering is introduced, the intranuclear cascades become more complex and, as a result, the excitation energies increase. However, the maximum increase in the excitation energies is only ~14 MeV.

It should be noted that the $\bar{E}^*_C$ values are a factor of 3 to 4 larger than the corresponding values of $\bar{E}^*_{N.C.}$. Furthermore, the fraction of the incident total energy which is retained as excitation energy in capture events is remarkably independent of the bombarding energy; the ISONEX-NO model predicts that ~36% of the total incident pion energy is retained as excitation energy when capture occurs in $^{209}$Bi. As one would expect, this fraction decreases as the mass of the target decreases; for $^{65}$Cu the ISONEX-NO model prediction for this fraction decreases to ~26%.

### C. Spallation Reactions

One of the principal goals of this calculation is the correct prediction of spallation product yields for a wide variety of targets and incident energies. As is well know, such predictions depend not only on the intranuclear cascade model used, but also on the manner in which the evaporation calcula-

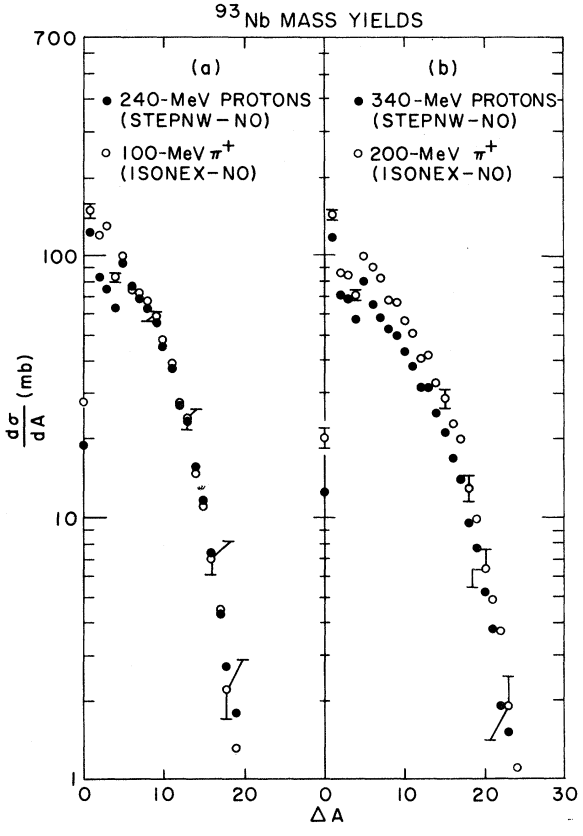


FIG. 5. Calculated mass yields for the interactions of (a) 240-MeV protons and 100-MeV $\pi^+$ and of (b) 340-MeV protons and 200-MeV $\pi^+$ with $^{93}$Nb.

tions are performed. In the present instance, the evaporation calculations were done with a code described by Dostrovsky *et al.*[15]

The predicted mass yields will first be discussed, since they are less dependent upon the evaporation calculations than are the individual product yields. No comparisons of calculated mass yields with experiment can be made since, as yet, experimental results do not exist.

On the basis of some early experiments with low-energy pions, it was concluded that the yield distributions from pion-induced reactions should be comparable to those for nucleons with kinetic energy equal to the total energy of the incident pion.[16] Hence, it is of interest to examine the validity of this conjecture. In Fig. 5 the calculated mass yields for the interactions of 240-MeV (340-MeV) protons and of 100-MeV (200-MeV) $\pi^+$ with $^{93}$Nb are compared. Similar comparisons are presented in Fig. 6 for the interactions of 240-MeV (375-MeV) protons and 100-MeV (250-MeV) $\pi^+$ with $^{209}$Bi. The STEPNW-NO model which is referred to in Figs. 5 and 6 is the STEPNO model described in Ref. 9 with the improved nucleon density distribution discussed in Ref. 17. In each of these four comparisons the proton results agree at least qualitatively with the corresponding $\pi^+$ results. That is, in each case both results span the same mass range and the difference between the pion and proton production cross sections for a given mass is less than a factor of 2. There are two barely statistically significant trends visible. The production cross sections are higher for pions than for protons at low bombarding energies for masses near the target and at high bombarding energies for masses far removed from the target. It will be interesting to see whether or not these trends also appear in experi-

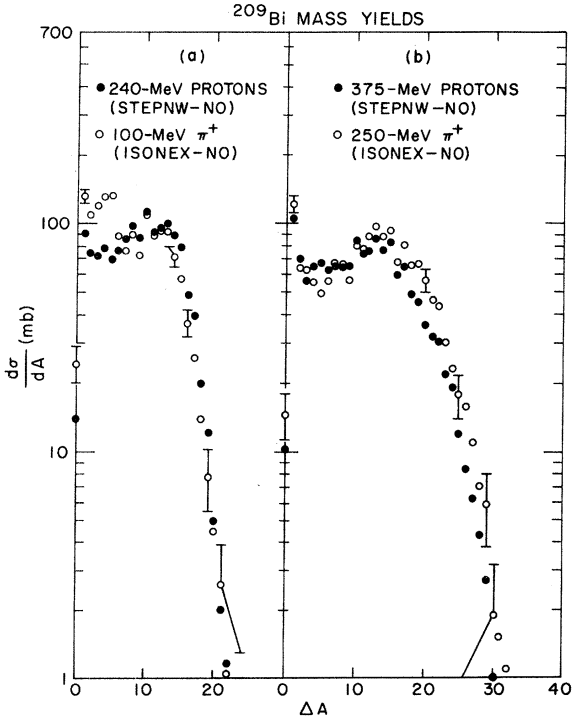


FIG. 6. Calculated mass yields for the interactions of (a) 240-MeV protons and 100-MeV $\pi^+$ and (b) 375-MeV protons and 250-MeV $\pi^+$ with $^{209}$Bi.

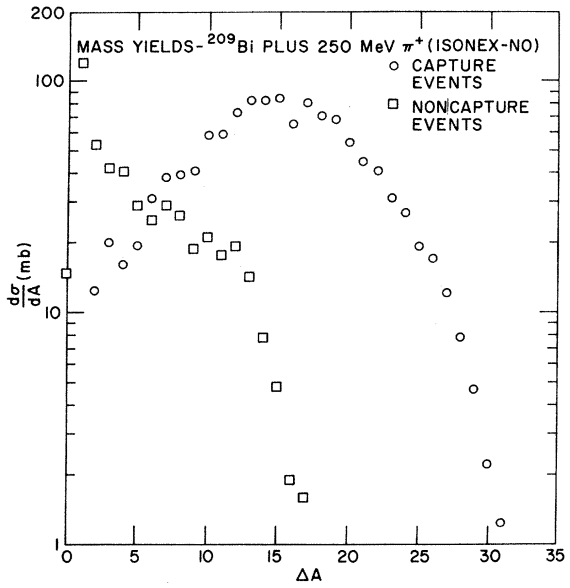


FIG. 7. Calculated mass yields from capture and noncapture events for the interaction of 250-MeV $\pi^+$ with $^{209}$Bi.

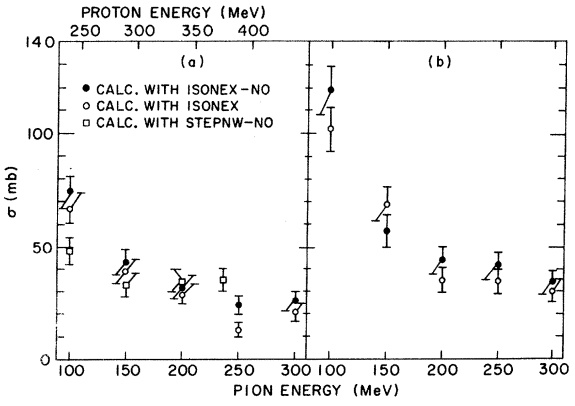


FIG. 8. Calculated excitation functions for the production of $^{206}$Bi by (a) positive pion and proton and (b) negative pion bombardment of $^{209}$Bi. The open squares are the proton results. Note the difference between the proton and pion bombarding energies.

mental results.

Calculated mass yields may be viewed as rather crude, physical measures of the excitation energy distributions of residual nuclei produced in the cascade process. Hence, from the discussion in Sec. III B one might expect that if one did evaporation calculations on residual nuclei produced in capture and noncapture events, separately, then the resulting mass yields would be quite different. In Fig. 7 the calculated mass yield for the interaction of 250-MeV $\pi^+$ with $^{209}$Bi is decomposed in precisely this manner and the results are indeed different for the two modes of pion-nucleus energy transfer. In particular, noncapture events are responsible for the production of nuclei near the target while capture events are responsible for the production of nuclei far removed from the target. Experiments to test this prediction will not be easy to design.

Predicted excitation functions for the production of $^{206}$Bi and $^{199}$Pb from the interaction of both positive and negative pions with $^{209}$Bi are given in Figs. 8 and 9. $^{206}$Bi is formed predominantly from nuclei produced in noncapture while $^{199}$Pb is predominantly formed from nuclei produced in capture events. The general form of these excitation functions is qualitatively the same for both positive and negative pions. That is, for both types of pions the cross section for $^{206}$Bi formation drops significantly with increasing bombarding energy while the cross section for $^{199}$Pb is fairly constant over the entire energy range. Also shown in Figs. 8(a) and 9(a) are the calculated excitation functions for the formation of $^{206}$Bi and $^{199}$Pb by proton bombardment of $^{209}$Bi. These two excitation functions agree fairly well with the corresponding results

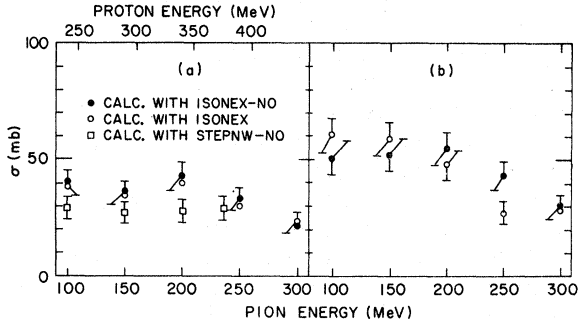


FIG. 9. Calculated excitation function for the production of $^{199}$Pb by (a) positive pion and proton and (b) negative pion bombardment of $^{209}$Bi. The open squares are the proton results. Note the difference between the proton and pion bombarding energies.

for positive pions. However, note that the proton bombarding energies are 140 MeV greater than the corresponding pion energies. If the proton and pion results for the production of $^{199}$Pb were compared at the same incident energies, the calculated cross sections would not agree nearly so well. For example, for incident protons the cross section for $^{199}$Pb formation increases from ~17 mb at 100 MeV to ~35 mb at 150 MeV, while for incident pions this cross section is essentially constant in this energy region (see Fig. 8).

From the discussion in Sec. III B, one would expect that isobar-nucleon "exchange" scattering should have its largest effect for high-energy negative pions on $^{209}$Bi. However, "exchange" scattering has no statistically significant effect on either of these negative pion excitation functions nor does it have a statistically significant effect on the calculated mass yields for the inter-

TABLE V. Calculated and experimental [a] spallation yields for the interaction of 65-MeV pions with Cu. All cross sections are in mb.

| Nuclide | $\pi^+$ Experimental | $\pi^+$ Calculated | $\pi^-$ Experimental | $\pi^-$ Calculated |
|---|---|---|---|---|
| $^{62}$Zn | 2.2 ± 0.6 | 6.1 ± 1.0 | . . . | . . . |
| $^{57}$Ni | 4.0 ± 1.4 | 4.7 ± 0.9 | 0.60 ± 0.15 | 0.47 ± 0.27 |
| $^{52}$Fe | 0.54 ± 0.17 | 1.0 ± 0.40 | 0.051 ± 0.015 | 0.15 ± 0.15 |
| $^{59}$Fe | 0.50 ± 0.15 | 1.4 ± 0.4 | 0.91 ± 0.28 | 9.0 ± 1.2 |
| $^{51}$Mn | 6.2 ± 1.8 | 4.3 ± 0.8 | 1.4 ± 0.8 | 1.2 ± 0.4 |
| $^{52}$Mn | 9.4 ± 2.5 | 18.0 ± 2.0 | 4.8 ± 1.3 | 10.1 ± 1.3 |
| $^{56}$Mn | 2.7 ± 0.7 | 1.3 ± 0.4 | 12.0 ± 2.4 | 8.8 ± 1.2 |
| $^{45}$Ti | 0.43 ± 0.13 | 0.37 ± 0.24 | 0.26 ± 0.06 | 0.12 ± 0.14 |
| ($^{43}$Sc + $^{44}$Sc) | 1.2 ± 0.4 | 0.20 ± 0.15 [b] | 0.30 ± 0.15 | 0.07 ± 0.08 [c] |
| $^{46}$Sc | 4.6 ± 1.3 | 0.33 ± 0.23 | 2.2 ± 0.8 | 0.85 ± 0.37 |
| [Sc] [c] | 1.4 ± 0.5 | 0.53 ± 0.30 [b] | 1.0 ± 0.5 | 3.0 ± 0.8 [c] |

[a] The experimental data are taken from Ref. 18. The experimental errors include the errors in the cross sections of the reference isotope, $^{56}$Mn.

[b] 50% of the $^{44}$Sc cross section was allocated to ($^{43}$Sc + $^{44}$Sc) and 50% to [Sc].

[c] [Sc] = $1.1\sigma(^{44}\mathrm{Sc}^m) + \sigma(^{47}\mathrm{Sc}) + 1.5\sigma(^{48}\mathrm{Sc})$.

action of 300-MeV $\pi^-$ with $^{209}$Bi.

In Table V the recent experimental results of Garrett and Turkevich[18] for the spallation of Cu by 65-MeV pions are compared to the corresponding calculated results. The calculated results are in fair to excellent agreement with experiment except for the production of $^{59}$Fe by negative pions and the production of $^{46}$Sc by positive pions. It is interesting to note that the calculated results for 65-MeV positive pions are essentially the same as those obtained from a similar calculation for the spallation of Cu by 205-MeV protons. Clearly, other spallation product yields would be of value in establishing the general usefulness of the present model in predicting such quantities.

### D. Spectra of Cascade Nucleons

One of the most stringent tests of intranuclear cascade models for high-energy incident nucleons is the correct prediction of the energy and angular distributions of directly emitted nucleons. As will be shown in the following, this is also true for intranuclear cascade calculations done with incident pions.

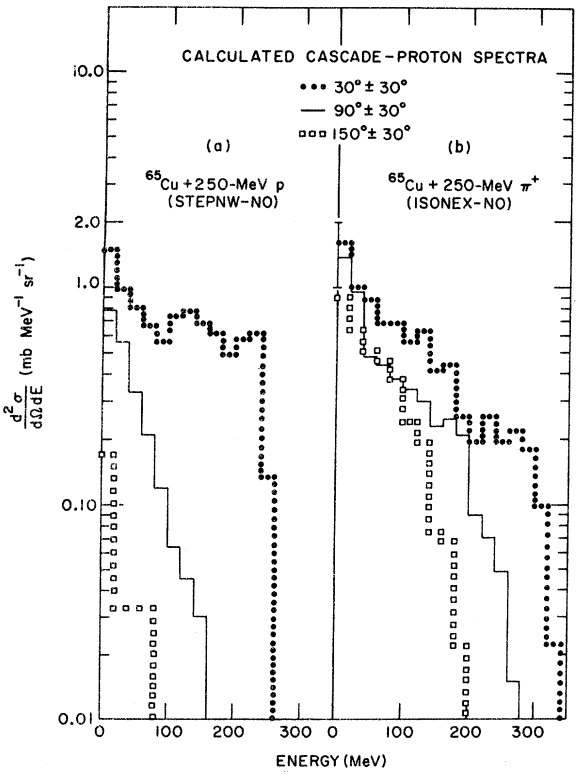


FIG. 10. Calculated energy spectra of protons emitted in the interaction of (a) 250-MeV protons and (b) 250-MeV $\pi^+$ with $^{65}$Cu.

In view of the lack of experimental data, it is interesting to compare calculated cascade-proton spectra for incident protons with similar spectra for incident pions. In Fig. 10 such a comparison is made between the emitted proton spectra obtained from the interactions of 250-MeV protons and 250-MeV $\pi^+$ with $^{65}$Cu. There are a number of points illustrated in this figure. Perhaps the most important one is that for incident pions one observes the emission of high-energy protons in all directions, while for incident protons the high energy protons are essentially confined to the forward direction. In addition, in the spectra for incident pions, one observes the emission of protons whose kinetic energies are greater than the kinetic energy of the incident pion.

Clearly, both of these observations are indicative of in-flight pion capture. This point is emphasized in Fig. 11 where the total proton spectrum at 90° is compared with the spectrum of protons from noncapture events only, at the same angle. It is obvious that the high-energy protons are produced solely by pion capture. Hence, a quantitative experimental measurement of the proton energy spectrum for ~200-MeV to ~300-MeV incident pions on medium nuclei would provide a severe test of the pion-capture mechanism employed in the present model. Positive pions would be more suitable for this experiment than nega-

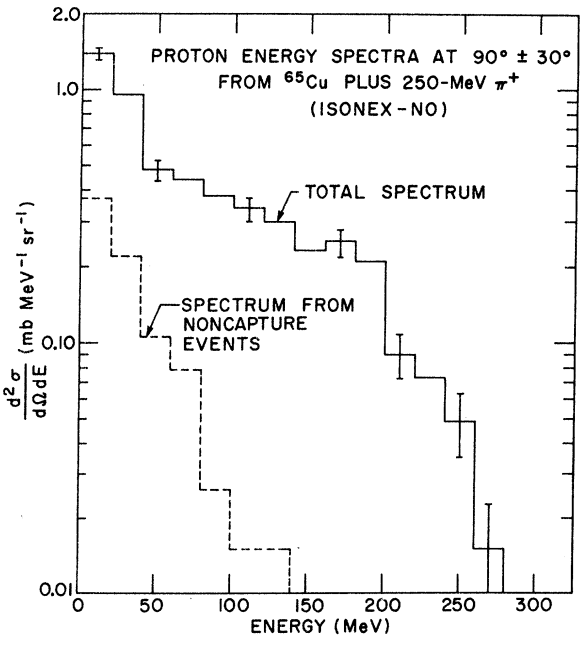


FIG. 11. Calculated energy spectrum of all protons emitted at 90° in the interaction of 250-MeV $\pi^+$ with $^{65}$Cu and the energy spectrum of protons emitted in noncapture events only.

tive pions, since the former produce more protons in capture than the latter. That is, in the present model

$$\frac{\sigma(\pi^+, 2p)}{\sigma(\pi^+, np)} \sim \frac{5Z}{N},$$

whereas

$$\frac{\sigma(\pi^-, 2n)}{\sigma(\pi^-, np)} \sim \frac{5N}{Z}, \tag{5}$$

where $N$ is the number of neutrons in the target. The above ratios were calculated assuming that the incident pion was absorbed and that the two nucleons escaped without further interactions.

Experimental measurements of nucleon energy spectra at higher pion bombarding energies would also be valuable as an indication of whether pion capture may take place through the interaction of elastically produced $T = \frac{1}{2}$ isobars with nucleons.

### E. Linear Momentum Transfer

The correlation between the average linear momentum of cascade products and their excitation energy is of considerable importance in the interpretation of recoil experiments.[19] This correlation has been studied extensively in simulations involving incident nucleons.[9] Hence, it is of interest to see of any significant differences arise when the projectile is changed from a nucleon to a pion.

For incident nucleons, it was found[9] that the average forward momentum transfer $\bar{p}_\parallel$ was approximately related to the excitation energy $E^*$ by $\bar{p}_\parallel/p_{\text{inc}} = E^*/E^*_{\text{max}}$ where $p_{\text{inc}}$ is the incident momentum and $E^*_{\text{max}}$ is the excitation energy of a compound nucleus. This is illustrated in Fig. 12 where $\bar{p}_\parallel/p_{\text{inc}}$ is plotted against $E^*/E^*_{\text{max}}$ for the interaction of 375-MeV protons with $^{209}$Bi. It was also found that this relation was practically independent of the target, projectile energy, and model used in these calculations.[9]

For incident pions, the dependence of $\bar{p}_\parallel$ on $E^*$ is not nearly so well defined because the distributions of momentum transfer for a given excitation energy interval are extremely broad. This is il-

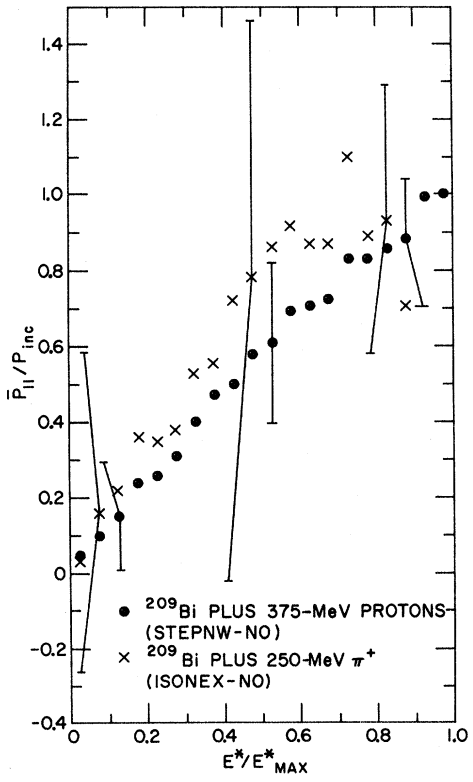


FIG. 12. Comparison of the $\bar{p}_\parallel/p_{\text{inc}}$ versus $E^*/E^*_{\text{max}}$ correlations for cascade products produced in the interactions of 375-MeV protons and 250-MeV $\pi^+$ with $^{209}$Bi. The root-mean-square deviations of the distributions are shown for some points.

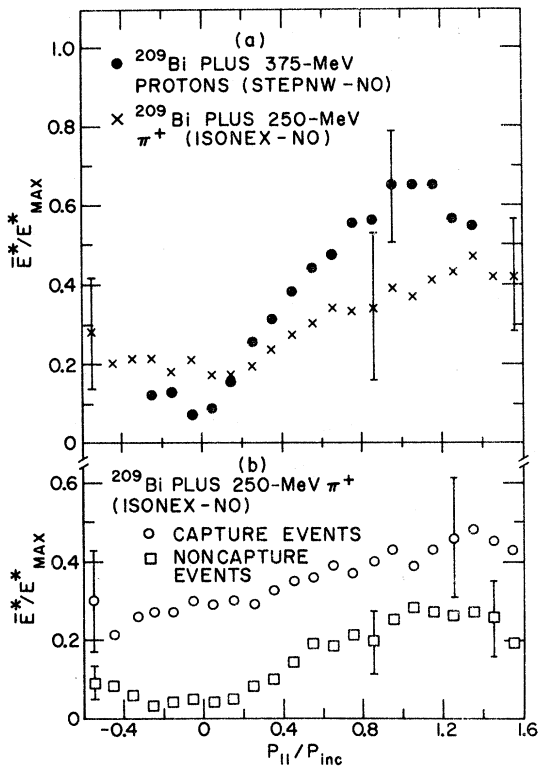


FIG. 13. $E^*/E^*_{\text{max}}$ versus $p_\parallel/p_{\text{inc}}$ correlations for (a) all cascade products produced in the interactions of 375-MeV protons and 250-MeV $\pi^+$ with $^{209}$Bi and for (b) cascade products produced in capture and noncapture events in the interaction of 250-MeV $\pi^+$ with $^{209}$Bi. The root-mean-square deviations of the distributions are shown for some points.

lustrated in Fig. 12 where the rms deviations of the $p_{\parallel}$ distributions (indicated by error bars) as well as the correlation between $\bar{p}_{\parallel}$ and $E^*$ for the interaction of 250-MeV $\pi^+$ with $^{209}$Bi are shown. The broad $p_{\parallel}$ distributions reflect the large variations in recoil momentum that accompany cascade nucleon emission.

The average excitation energy is less dependent on the forward momentum transfer for incident pions than for incident nucleons. This is illustrated in Fig. 13(a) where $\bar{E}^*/E^*_{\max}$ is plotted against $p_{\parallel}/p_{\text{inc}}$ for 375-MeV protons and 250-MeV $\pi^+$ on $^{209}$Bi. Note that for pions, the distributions of excitation energy for a given momentum transfer interval are much narrower than the distributions of momentum transfer for a given excitation energy interval.

In Fig. 13(b) the $\bar{E}^*$ versus $p_{\parallel}$ relations for residual nuclei formed in capture and noncapture events in the interaction of 250-MeV $\pi^+$ with $^{209}$Bi are compared. It is not too surprising that, for a given momentum transfer, the average excitation energy from capture is larger than the average excitation energy from noncapture. Note that for capture events, $\bar{E}^*$ shows only a slight, approximately linear, increase with $p_{\parallel}$.

### F. $^{12}C(\pi^-,\pi^- n)^{11}C$ Reaction

In Fig. 14 the calculated and experimental[20] excitation functions for the $^{12}C(\pi^-, \pi^- n)^{11}C$ reaction are compared. The results calculated with the ISONEX-NO model are in fair agreement with experiment. The introduction of isobar-nucleon "exchange" scattering causes only minor changes in the calculated results.

## IV. SUMMARY AND CONCLUSIONS

The effects of including the production and subsequent interactions of (3, 3) isobars in intranuclear cascade studies of low-energy pion-induced reactions have been studied. Isobar-nucleon "exchange" scattering, one of the two assumed isobar-nucleon reaction mechanisms, was shown to have very little effect on the calculated results, despite the large cross sections for this process. On the other hand, the energy dependence of pion-nucleus reaction cross sections and the energy spectra of inelastically scattered pions were found to be sensitive to the pion-nucleus potential assumed in these calculations.

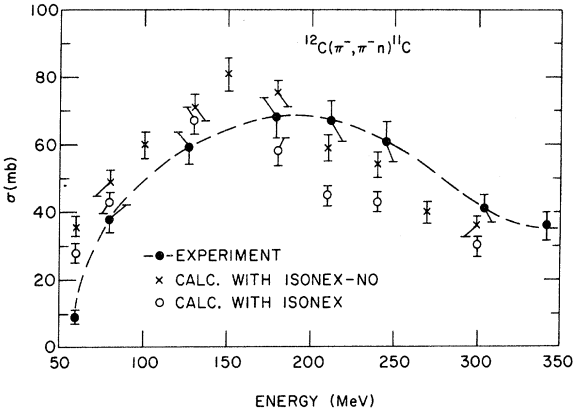


FIG. 14. Excitation function for the production of $^{11}C$ by negative pion bombardment of $^{12}C$. The experimental data are taken from Ref. 20.

Calculated mass yields for pion-induced reactions were compared with those for nucleon-induced reactions. The results for the two types of particle were at least qualitatively in agreement when the kinetic energies of the incident nucleons were equal to the total energies of the incident pions. Consistent differences were found for masses near the target at low bombarding energies and for masses far removed from the target at high bombarding energies. In both instances the production cross sections for pions were higher than for nucleons.

At present it is difficult to test the validity of some of the assumptions made in the present model or to determine the general applicability of the model. However, this situation will soon change when intense pion beams become available.

## ACKNOWLEDGMENTS

Helpful discussions with many colleagues, in particular with Dr. W. Rubinson, Dr. J. Hudis, Dr. R. Sternheimer, Dr. J. Cumming, and Dr. L. Remsberg, are gratefully acknowledged. The authors would also like to thank the staff of the Brookhaven computing center for their generous cooperation and advice and Mrs. M. Kinney for her assistance in the data reduction.

*Research supported by the U. S. Atomic Energy Commission.

[1]R. M. Sternheimer and S. J. Lindenbaum, Phys. Rev. **123**, 333 (1961); Phys. Rev. **109**, 1723 (1958); Phys. Rev. **105**, 1874 (1957).
[2]H. W. Bertini, Phys. Rev. **188**, 1711 (1969); Phys. Rev. C **6**, 631 (1972).
[3]S. L. Whetstone, Los Alamos Report No. LA-3206-MS, 1963 (unpublished).
[4]H. W. Bertini, Phys. Rev. **131**, 1801 (1963).
[5]N. Metropolis *et al.*, Phys. Rev. **110**, 204 (1958).
[6]V. Barashenkov *et al.*, Acta Phys. Pol. **36**, 457 (1969).
[7]Z. Fraenkel, Phys. Rev. **130**, 2407 (1963).

[8]Z. Fraenkel, Nuovo Cimento **30,** 512 (1963).
[9]K. Chen *et al.*, Phys. Rev. **166,** 949 (1968).
[10]K. Chen *et al.*, Phys. Rev. C **4,** 2234 (1971).
[11]L. Kisslinger, Phys. Rev. **98,** 761 (1955).
[12]G. Giacomelli *et al.*, Cern Report No. CERN/HERA 69-1, 1969 (unpublished).
[13]F. Binon *et al.*, Nucl. Phys. **B17,** 168 (1970).
[14]B. Nikol'skii *et al.*, Zh. Eksp. Teor. Fiz. 32, 48 (1957) [Sov. Phys.-JETP 5, 93 (1957)].
[15]I. Dostrovsky *et al.*, Phys. Rev. **116,** 683 (1959).
[16]J. Hudis in *Nuclear Chemistry*, edited by L. Yaffe (Academic, New York, 1968), Vol. I.
[17]K. Chen *et al.*, Phys. Rev. **176,** 1208 (1968).
[19]C. K. Garrett and A. Turkevich, Phys. Rev. C 8, 594 (1973).
[19]See e.g., V. Crespo *et. al.*, Phys. Rev. **131,** 1765 (1963); J. B. Cumming *et al.*, Phys. Rev. 134, B1262 (1964); J. Alexander in *Nuclear Chemistry*, edited by L. Yaffe (Academic, New York, 1968), Vol. I.
[20]P. Reeder and S. Markowitz, Phys. Rev. 133, B639 (1964).